

Understanding the Absorption of Fluorinated Gases in Fluorinated Ionic Liquids for Recovering Purposes Using Soft-SAFT

Margarida L. Ferreira, João M. M. Araújo, Lourdes F. Vega,* and Ana B. Pereira*

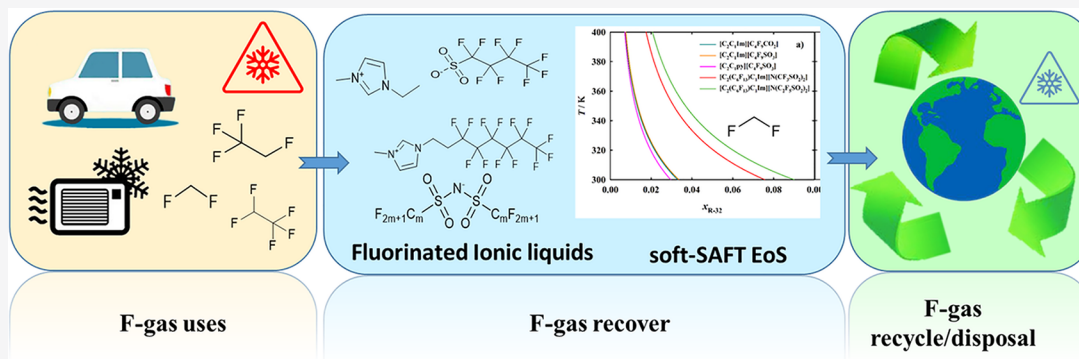
Cite This: <https://doi.org/10.1021/acs.jced.1c00984>

Read Online

ACCESS |

Metrics & More

Article Recommendations



ABSTRACT: It is proven that fluorinated gases (F-gases) have a vast impact on climate change due to their high global warming potential. Hence, it is imperative to search for new molecules to replace them in current applications, as well as technologies to capture, recover, and recycle F-gases to avoid their emissions to the atmosphere. One of the attractive technologies for this purpose is to absorb them in fluorinated ionic liquids (FILs), given their solubilization power. However, the complexity of FILs and the time-consuming experimental methodologies to fully characterize them hinder their prompt usage in this urgent field. In this work, the soft-Statistical Associating Fluid Theory (soft-SAFT) Equation of State is used as a tool to investigate the solubility of six different F-gases (R-32, R-125, R-134a, R-14, R-116, R-218) in five FILs ($[\text{C}_2\text{C}_1\text{Im}][\text{C}_4\text{F}_9\text{SO}_3]$, $[\text{C}_2\text{C}_1\text{Im}][\text{C}_4\text{F}_9\text{CO}_2]$, $[\text{C}_2\text{C}_1\text{py}][\text{C}_4\text{F}_9\text{SO}_3]$, $[\text{C}_2(\text{C}_6\text{F}_{13})\text{C}_1\text{Im}][\text{N}(\text{CF}_3\text{SO}_2)_2]$, and $[\text{C}_2(\text{C}_6\text{F}_{13})\text{C}_1\text{Im}][\text{N}(\text{C}_2\text{F}_5\text{SO}_2)_2]$). The robustness of the soft-SAFT approach allowed the establishment of new FIL models in a simple and fast way, and the calculation of F-gases solubility in them, in excellent agreement with existing experimental data. Once the models were assessed, a systematic study was performed regarding the structural features of FILs favoring their performance to absorb F-gases by using the soft-SAFT approach as a screening tool. It has been obtained that the solubility is favored by the presence of a perfluoroalkyl chain in the imidazolium cation, together with a bulkier anion. In all cases, $[\text{C}_2(\text{C}_6\text{F}_{13})\text{C}_1\text{Im}][\text{N}(\text{C}_2\text{F}_5\text{SO}_2)_2]$ shows a superior solubility of F-gases than the $[\text{C}_2(\text{C}_6\text{F}_{13})\text{C}_1\text{Im}][\text{N}(\text{CF}_3\text{SO}_2)_2]$, also indicating that the addition of one carbon to the two anionic symmetric fluorinated chains contributes to the gas-philicity of the FILs. This work proves the relevance of using the soft-SAFT framework to obtain insights into the behavior of such complex systems and key trends, even when experimental data are scarce, as a step forward in assessing systems for separating and recovering F-gases.

INTRODUCTION

In the last recent years, climate change has become one of the main concerns of all nations, due to the registered high temperatures and weather pattern shifts occurring worldwide, drastically affecting the way of living on the planet.¹ The current headlines on the daily news show the massive effects of global warming by the successive tragic events such as floods, droughts, wildfires, and hurricanes which have caused thousands of deaths, displacement of the people, and high economic losses.^{1,2} One of the main reasons of global warming is the emission of greenhouse gases (GHGs) to the atmosphere. The concentration of GHGs has attained the highest levels in 2 million years, and the emissions are still rising;¹ hence, it must be drastically reduced in order to leave a

habitable world for future generations. The main atmospheric gases emitted are carbon dioxide, methane, and nitrous oxide, with annual averages in 2019 of 410 ppm, 1866 ppb, and 332 ppb, respectively,³ well above their values before 1850. In addition to atmospheric GHG, other GHGs exclusively resulting from human activities are also emitted, such as

Special Issue: In Honor of Joan F. Brennecke

Received: December 28, 2021

Accepted: March 25, 2022

fluorinated gases (F-gases), of major concern due to their huge global warming potential (GWP), thousands of times greater than that of CO₂.⁴ F-gases are mainly used in refrigeration, air conditioning, heat equipment, and electrical sectors.^{5,6} The increased usage of F-gases in cooling systems is a result of a complete substitution of ozone-depleting substances such as chlorofluorocarbons (CFCs) and hydrochlorofluorocarbons (HCFCs) as imposed by the Montreal Protocol in 1987.⁷ Once CFCs were forbidden, F-gases started to be massively used, reaching concentrations in the atmosphere in 2019 of 109, 10, 2, and 237 ppt for perfluorocarbons (PFCs), sulfur hexafluoride (SF₆), nitrogen trifluoride (NF₃), and hydrofluorocarbons (HFCs), respectively.³ Therefore, the Kyoto Protocol was established to regulate and control the usage of GHGs, including F-gases, limiting their emissions.⁸ In 2016, Kigali's amendment to the Montreal Protocol was introduced and entered into force in 2019. It was the first global agreement to reduce F-gases emissions.⁹ Other regulations are in place, for instance, the European Union (EU) legislation (EU No. 517/2014), aiming for the reduction of F-gases emissions by two-thirds by 2030.¹⁰

To properly fulfill the phase-out of F-gases imposed by these regulations, it is of great importance to find new molecules or blends to replace these high GWP compounds,¹¹ as well as to develop new and sustainable technologies, based on the circular economy, to ease the capture, recover, and recycle of the F-gases used in the refrigeration sector. This will enable the reduction of their destruction, which is executed by incineration, resulting in higher emissions.^{5,12} Furthermore, refrigeration and air conditioning systems must be improved to prevent the leakage of refrigerants into the atmosphere.^{5,12}

Different strategies are envisioned to capture and separate F-gases before they are emitted into the atmosphere. Among them, ionic liquids (ILs) are compounds with very attractive properties to be applied in the capture and recovery of different gases,^{13–15} and are recently being studied for this purpose. ILs can be fine-tuned by the selection of the counterions, which enables the design of an IL with specific properties for a target application. Great advances have been made in this field in the last years since the pioneering work, and further contributions, of Brennecke and collaborators,¹⁶ who have set up the methodological procedures to understand and characterize ILs, as well as the design of these solvents for different applications.^{17,18} From a historical viewpoint, the reader is referred to the visionary perspective article Brennecke and Maginn, published back in 2001, on the potential applications of ILs.¹⁹

Recently, fluorinated ionic liquids (FILs), defined in this work as ILs with anionic and/or cationic perfluoroalkyl chains with a minimum of four carbons, have received great attention in the solvation of fluorine compounds.^{20–22} They are considered three-in-one solvents due to the formation of three nanosegregated domains (polar, hydrogenous, and fluorous).^{23–26} This enhanced solubilization power, combined with the increased free volume due to the asymmetry between the counterions, size of the fluorinated chains, and its rigidity resulting from the strong carbon–fluorine bonds,^{22–25,27,28} makes FILs appealing compounds for F-gases applications. Their improved properties are found by gathering the best of the conventional ILs (insignificant vapor pressure, superior thermal stability, diminished flammability, and easy recovery and recycling) with the characteristic chemical and biological inertness, low surface tension, and superior surfactant behavior

of the perfluoroalkyl compounds.^{22,25–34} For instance, FILs based on perfluoroalkyl chains composed of four carbons can have total miscibility in water,^{32–34} superior aggregation behavior by the formation of different stable self-assembled structures in aqueous solutions,^{31–34} and negligible cytotoxicity^{35–37} and ecotoxicity.^{38,39} Therefore, it is possible to design *ad-hoc* FILs with improved ability to absorb F-gases, and with intrinsic properties that comply with the principles of green chemistry and sustainability.

In spite of the highlighted relevance, few works have focused so far on the determination of F-gases absorption by FILs. Sosa et al.⁴⁰ determined the solubility of several HFCs in FILs containing perfluorobutanesulfonate and perfluoropentanoate anions, showing the importance of the fluorine content and nanosegregated domains in the absorption of F-gases. Lepre and co-workers^{41,42} studied the behavior of a HFC and different PFCs in the presence of FILs with cationic perfluoroalkyl chains with six carbon atoms, obtaining a positive correlation between the presence of cationic fluorine content and the solubilization of F-gases.^{41,42} Castro et al.⁴³ and Jovell et al.⁴⁴ successfully studied the solubilization of HFCs in FILs and deep eutectic solvents (DESs) based on mixtures of FILs and perfluoroalkyl acids.

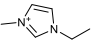
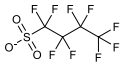
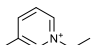

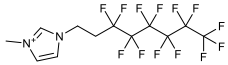
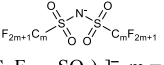


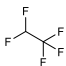
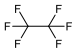
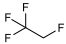
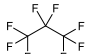
The large number of FILs that can be synthesized by different cations/anions combinations turns the experimental determination of their properties into an arduous and cost-consuming task. Therefore, the use of models able to predict the absorption of F-gases by FILs is of great importance to accelerate their actual implementation. Different tools can be used for this purpose, such as molecular simulation approaches, correlative methods, and equations of state.^{13–15,45,46} Pereiro and co-workers contributed to the development of new technologies to alleviate the environmental impact of F-gases with the support of modeling approaches such as the COSMO-based/Aspen Plus methodology and nonrandom two-liquid (NRTL) models.^{44,43,47} The soft-SAFT EoS, proposed by Blas and Vega,^{48,49} extensively used to study the gas solubility in complex systems, including ILs and DES,^{28,44–46,50–59} has also been used to describe the solubility of selected F-gases in ILs.^{60–62} Of particular interest to this contribution is the recent work by Albà et al.,⁵⁷ modeling FILs for selectively separating hydrofluoroolefins (HFOs) from HFCs from the azeotropic blend R513A. Jovell et al.⁴⁴ also used soft-SAFT to model the solubility of R134a in FILs and DES based on perfluoroalkyl acid, but much work remains to be done. Building on previous works, in this contribution we apply the soft-SAFT framework to predict the solubility of selected F-gases in FILs, searching for trends between their molecular structure and their final performance.

METHODOLOGY

The soft-SAFT EoS^{48,49} is a well-known version of the original SAFT EoS,^{63–65} widely used for the description of complex systems. Literature corroborates soft-SAFT as a great tool to accurately provide the properties and phase behavior of ILs and their mixtures with other substances such as water, gases, and/or other ILs in good agreement with experimental data.^{28,29,34,44,46,50,51,53}

All SAFT equations describe the fluids by a chain of interconnected spheres and are expressed as the sum of the different contributions to the residual Helmholtz energy (A^{res}) of a neat fluid:

Table 1. Structure and Nomenclatures of the Cations and Anions Composing the Ionic Liquids, and the Fluorinated Gases Studied in This Work

Cations	Anions
 $[C_2C_1Im]^+$ 1-Ethyl-3-methylimidazolium	 $[C_4F_9SO_3]^-$ Perfluorobutanesulfonate
 $[C_2C_1py]^+$ 1-Ethyl-3-methylpyridinium	 $[C_4F_9CO_2]^-$ Perfluoropentanoate
 $[C_2(C_6F_{13})C_1Im]^+$ 1-(3,3,4,4,5,5,6,6,7,7,8,8,8-Tridecafluorooctyl)-3-methylimidazolium	 $[N(C_mF_{2m+1}SO_2)_2]^-$, $m = 1, 2$ Bis(perfluoroalkylsulfonyl)imide
Fluorinated Gases	
 R-32 (CH_2F_2) Difluoromethane	 R-14 (CF_4) Tetrafluoromethane
 R-125 (C_2HF_5) Pentafluoroethane	 R-116 (C_2F_6) Hexafluoroethane
 R-134a ($C_2H_2F_4$) 1,1,1,2-Tetrafluoroethane	 R-218 (C_3F_8) Octafluoropropane

$$A^{\text{res}} = A^{\text{ref}} + A^{\text{chain}} + A^{\text{assoc}} + A^{\text{polar}} \quad (1)$$

The A^{ref} accounts for the reference term, which in soft-SAFT is ruled by a Lennard-Jones (LJ) intermolecular potential taking into account dispersive and repulsive interactions between the monomers (groups) forming the molecules.⁶⁶ The A^{chain} term accounts for the formation of the chain from the monomers, A^{assoc} represents the site–site intermolecular associations between the monomers composing the coarse-grained model for the case of associating fluids, chain and association terms being directly derived from the Wertheim's first-order thermodynamic perturbation theory.^{67–70} Finally, A^{polar} explicitly takes into account the polar interactions for dipolar and quadrupolar fluids.^{71,72} Consequently, nonpolar, associating fluids are modeled within the soft-SAFT framework by using a coarse-grained model characterized by a set of molecular parameters that describe the structural features and interactions of the fluids. Nonassociating fluids need three molecular parameters, namely, m , the chain length, σ , the segment diameter of the monomers integrating the chain and, ϵ , the dispersive energy between the monomers. For associating fluids, two additional parameters are considered to describe the associating interactions, the site–site association energy, ϵ^{HB} , and one related to the site–site bonding-volume of association, κ^{HB} .

The chain and association terms in soft-SAFT are readily applicable to mixtures, while the generalized Lorentz–Berthelot mixing rules are used to calculate the binary

parameters describing the size ($\eta_{ij} = \eta$) and energy ($\xi_{ij} = \xi$) asymmetries between the monomers integrating the different fluids on a mixture in the A^{ref} term in eq 1, as:

$$\sigma_{ij} = \eta_{ij} \left(\frac{\sigma_{ii} + \sigma_{jj}}{2} \right) \quad (2)$$

$$\epsilon_{ij} = \xi_{ij} \sqrt{\epsilon_{ii} \epsilon_{jj}} \quad (3)$$

The value of both binary parameters is unity when using the equation in a predictive manner. If the mixture studied is composed of two associating fluids, such as the ILs and the F-gases herein studied, the association energy ($\epsilon_{\alpha\beta,ij}^{\text{HB}}$) and volume ($\kappa_{\alpha\beta,ij}^{\text{HB}}$) parameters of the binary system must be calculated by the following rules:

$$\kappa_{\alpha\beta,ij}^{\text{HB}} = \left(\frac{\sqrt[3]{\kappa_{\alpha\beta,ii}^{\text{HB}}} + \sqrt[3]{\kappa_{\alpha\beta,jj}^{\text{HB}}}}{2} \right)^3 \quad (4)$$

$$\epsilon_{\alpha\beta,ij}^{\text{HB}} = \sqrt{\epsilon_{\alpha\beta,ii}^{\text{HB}} \epsilon_{\alpha\beta,jj}^{\text{HB}}} \quad (5)$$

The soft-SAFT model and corresponding software are readily available for phase equilibria calculations, and hence, solubility calculations, by imposing the equality of chemical potential of each component in the coexisting phases at fixed temperature and pressure, to satisfy chemical, thermal, and

Table 2. Molecular Weight, Soft-SAFT Molecular Parameters of Fluorinated Ionic Liquids and Fluorinated Gases from Literature and Optimized in This Work, and the Respective Absolute Average Deviation (AAD) of the Density Experimental Data⁴⁰

substance	M_w	m	σ	ϵ/k_B	ϵ^{HB}/k_B	κ^{HB}	AAD	ref
	$\text{g}\cdot\text{mol}^{-1}$		\AA	K	K	\AA^3	%	
Ionic Liquids								
[C ₂ C ₁ Im][C ₄ F ₉ CO ₂]	374.21	7.233	3.762	338.8	3850	2250		50
[C ₂ C ₁ Im][C ₄ F ₉ SO ₃]	410.31	7.320	3.816	343.4	3850	2250		28
[C ₂ C ₁ py][C ₄ F ₉ SO ₃]	421.28	7.320	3.889	359.4	3850	2250		50
[C ₁₁ C ₁ Im][N(CF ₃ SO ₂) ₂]	517.55	6.732	4.595	416.3	3450	2250		53
[C ₁₄ C ₁ Im][N(CF ₃ SO ₂) ₂]	559.54	6.967	4.731	422.7	3450	2250		53
[C ₂ (C ₆ F ₁₃)C ₁ Im][N(CF ₃ SO ₂) ₂]	709.34	6.518	4.595	343.7	3450	2250	0.013	this work
[C ₂ (C ₆ F ₁₃)C ₁ Im][N(C ₂ F ₅ SO ₂) ₂]	809.36	6.690	4.731	339.4	3450	2250	0.007	this work
Fluorinated Gases								
R-32 (CH ₂ F ₂)	52.02	1.321	3.529	144.4	1708	24050		51
R-125 (C ₂ HF ₅)	120.02	1.392	4.242	148.8	1685	24050		51
R-134a (C ₂ H ₂ F ₄)	102.03	1.392	4.166	166.6	1862	24050		62
R-14 (CF ₄)	88.00	1.000	4.217	190.1				61
R-116 (C ₂ F ₆)	138.01	1.392	4.342	204.5				61
R-218 (C ₃ F ₈)	188.02	1.776	4.399	214.7				61

mechanical stability. As the model is explicitly formulated in terms of temperature, density, and phase composition, the fugacity method is applied by equating chemical potential and pressure at a fixed temperature as:

$$\mu_i^I(T, \rho^I, x^I) = \mu_i^{II}(T, \rho^{II}, x^{II}) \quad (6)$$

$$P^I(T, \rho^I, x^I) = P^{II}(T, \rho^{II}, x^{II}) \quad (7)$$

The soft-SAFT EoS methodology has been already extensively described in the literature, and the reader is referred to previous works for further details.^{45,50,53,60–62}

Different thermodynamic parameters were considered and determined in the work, to further extract information on the interactions between the F-gases and the FILs, and hence, their solubility. This includes Henry constants, enthalpy and entropy of dissolution, and the Hildebrand solubility parameter. The Henry constants (H_c) were determined from the diagram of the pressure versus gas composition at two different temperatures. The values of H_c were obtained in the range of low gas composition (0.01 to 0.05 $x_{F\text{-gas}}$) corresponding to the infinite dilution of each VLE of FIL + F-gas as described by eq 8.

$$H_c = \lim_{x_{F\text{-gas}} \rightarrow 0} \left(\frac{P}{x_{F\text{-gas}}} \right) \quad (8)$$

The enthalpy ($\Delta_{\text{dis}}H$) and entropy ($\Delta_{\text{dis}}S$) of dissolution were also considered in this work to obtain information on the strength of the interactions and the degree of order of the F-gases dissolved in the FILs, respectively.⁵⁷ These two thermodynamic parameters were calculated by eqs 9 and 10.

$$\Delta_{\text{dis}}H = R \left| \frac{\Delta \ln H_c}{\Delta 1/T} \right|_{x_{\text{id}}}^{\infty} \quad (9)$$

$$\Delta_{\text{dis}}S = -R \left| \frac{\Delta \ln H_c}{\Delta \ln T} \right|_{x_{\text{id}}}^{\infty} \quad (10)$$

where T is the temperature of the system and x_{id} is the molar composition of the F-gas dissolved in the FIL at infinite dilution.

Finally, the Hildebrand solubility parameter (δ) was determined for each FIL and each F-gas. This parameter is obtained through the square root of the ratio between the energy of vaporization ($\Delta_{\text{vap}}U$) and the molar volume (v) as represented in eq 11.

$$\delta = \sqrt{\frac{\Delta_{\text{vap}}U}{v}} = \sqrt{\frac{\Delta_{\text{vap}}H - RT}{v}} \quad (11)$$

The $\Delta_{\text{vap}}U$ can be obtained through the enthalpy of vaporization ($\Delta_{\text{vap}}H$) as indicated in eq 11. Therefore, the $\Delta_{\text{vap}}H$ was determined in this work by predicting the vapor pressure of the pure systems, as indicated in eq 12.

$$\Delta_{\text{vap}}H = -R \left| \frac{\Delta \ln P}{\Delta 1/T} \right| \quad (12)$$

RESULTS AND DISCUSSION

The solubility of different F-gases in FILs has been studied in this work using soft-SAFT in order to extract insights into the relationship between the molecular structure and the solvation performance of these FILs. The selected F-gases are three PFCs (R-14, R-116, and R-218) and three HFCs (R-32, R-125, and R-134a), the chemical structures of which, containing from 2 to 8 fluorine atoms, are provided in Table 1. Besides, five FILs were chosen: two very similar ILs, (1) [C₂C₁Im]-[C₄F₉SO₃] and (2) [C₂C₁Im][C₄F₉CO₂], just replacing SO₃ in the anion in (1) by CO₂ in the anion of (2); (3) [C₂C₁py][C₄F₉SO₃], containing the same anion as (1) but changing the cation, (4) [C₂(C₆F₁₃)C₁Im][N(CF₃SO₂)₂], and (5) [C₂(C₆F₁₃)C₁Im][N(C₂F₅SO₂)₂] both with very bulky cations compared to 1–3, and in which the only difference between them is the number of fluorine atoms in the anion. Their nomenclature and structures can also be found in Table 1.

Soft-SAFT Coarse-Grained Molecular Models and Parametrization. Soft-SAFT characterizes the fluids by a coarse-grained model that must mimic the principal structural features and interactions of the fluids. As mentioned, nonassociating molecules are defined by three molecular parameters (m , σ , and ϵ). For associating fluids, an association

scheme must be delineated by selecting the number of association sites, defining the type of association that can occur between those sites, and characterizing them with two parameters, one representing the energy of the association sites (ϵ^{HB}) and the other one related to the volume of association (κ^{HB}). The models of F-gases considered in this work have been already established within the soft-SAFT framework and are used here in a transferable manner, without any refinement.^{51,60–62} PFCs are modeled as nonassociating homonuclear chains.⁶¹ In the soft-SAFT approach HFCs can be modeled as polar fluids (where the dipolar interactions are explicitly taken into account), or as associating fluids, where the dipolar interactions are considered in an implicit manner through the association term.⁷³ In this work, HFCs were modeled as associating molecules by adding two association sites (one negative and other positive) to the homonuclear chainlike model, to mimic the dipolar interactions from the fluorine electronegativity.⁶⁰ This model was chosen for consistency with previous works, where it was successfully used to describe the thermodynamic properties of HFCs, including the behavior with other ILs with the soft-SAFT approach.^{44,51,60,62} The molecular and association parameters of HFCs recently reparametrized^{51,62} have been used in this work and they are provided in Table 2 for completeness.

In soft-SAFT, ILs are modeled as associating chain molecules, considering the anion and the cation as an ion pair due to the reduced ionic character consequence of specific steric interactions, dispersion forces, and formation of short-lived ion pairs.^{28,29,34,44,45,50,51,53} The reader is referred to previous work for more details on modeling FILs within the soft-SAFT framework.²⁹ The soft-SAFT coarse-grain models of $[\text{C}_2\text{C}_1\text{Im}][\text{C}_4\text{F}_9\text{SO}_3]$, $[\text{C}_2\text{C}_1\text{Im}][\text{C}_4\text{F}_9\text{CO}_2]$, and $[\text{C}_2\text{C}_1\text{py}][\text{C}_4\text{F}_9\text{SO}_3]$ FILs^{28,50} already available in the literature were used in this work in a transferable manner. They were modeled with a three-site association scheme: one site named *A* to represent the interactions between the cation and anion and two sites *B* to account for the delocalization of charge due to the fluorinated alkyl chains. Only *AB* interactions are allowed in these models. The molecular and association parameters are in Table 2.

Conversely, $[\text{C}_2(\text{C}_6\text{F}_{13})\text{C}_1\text{Im}][\text{N}(\text{CF}_3\text{SO}_2)_2]$ and $[\text{C}_2(\text{C}_6\text{F}_{13})\text{C}_1\text{Im}][\text{N}(\text{C}_2\text{F}_5\text{SO}_2)_2]$ were modeled for the first time in this work. For consistency, the scheme of association for $[\text{C}_2(\text{C}_6\text{F}_{13})\text{C}_1\text{Im}][\text{N}(\text{CF}_3\text{SO}_2)_2]$ and $[\text{C}_2(\text{C}_6\text{F}_{13})\text{C}_1\text{Im}][\text{N}(\text{C}_2\text{F}_5\text{SO}_2)_2]$ was transferred from the $[\text{C}_n\text{C}_1\text{Im}][\text{N}(\text{CF}_3\text{SO}_2)_2]$ series.⁶⁰ Three association sites were included to describe the FIL interactions (one site *A* and two sites *B*) where only *AB* contacts are allowed: *A* site represents the interactions between the cation and the anionic nitrogen atom and the *B* sites are on behalf of the delocalized charge of the anion resulting from the oxygen groups. The approach for obtaining the molecular and association parameters consisted of transferring and optimizing the soft-SAFT parameters through the careful analysis of the FILs structural features.²⁹ The structures of both $[\text{C}_2(\text{C}_6\text{F}_{13})\text{C}_1\text{Im}][\text{N}(\text{CF}_3\text{SO}_2)_2]$ and $[\text{C}_2(\text{C}_6\text{F}_{13})\text{C}_1\text{Im}][\text{N}(\text{C}_2\text{F}_5\text{SO}_2)_2]$ FILs were evaluated in order to find a member of the $[\text{C}_n\text{C}_1\text{Im}][\text{N}(\text{CF}_3\text{SO}_2)_2]$ series similar in size and volume. The additional fluorine atoms were considered by choosing and transferring all the parameters of a member of $[\text{C}_n\text{C}_1\text{Im}][\text{N}(\text{CF}_3\text{SO}_2)_2]$ with longer hydrogenated chains, taking into account that one fluorine atom is approximately 1.5 times larger than a hydrogen atom.³² Therefore, the molecular parameters of $[\text{C}_{11}\text{C}_1\text{Im}][\text{N}(\text{CF}_3\text{SO}_2)_2]$ and $[\text{C}_{14}\text{C}_1\text{Im}][\text{N}(\text{CF}_3\text{SO}_2)_2]$ ⁶⁰ (see Table 2) were directly transferred to $[\text{C}_2(\text{C}_6\text{F}_{13})\text{C}_1\text{Im}][\text{N}(\text{CF}_3\text{SO}_2)_2]$ and $[\text{C}_2(\text{C}_6\text{F}_{13})\text{C}_1\text{Im}][\text{N}(\text{C}_2\text{F}_5\text{SO}_2)_2]$, respectively, without any adjustment to experimental data. The densities at atmospheric pressure were calculated with the soft-SAFT parameters of $[\text{C}_{11}\text{C}_1\text{Im}][\text{N}(\text{CF}_3\text{SO}_2)_2]$ and $[\text{C}_{14}\text{C}_1\text{Im}][\text{N}(\text{CF}_3\text{SO}_2)_2]$ and compared with the experimental data^{40,41} of $[\text{C}_2(\text{C}_6\text{F}_{13})\text{C}_1\text{Im}][\text{N}(\text{CF}_3\text{SO}_2)_2]$ and $[\text{C}_2(\text{C}_6\text{F}_{13})\text{C}_1\text{Im}][\text{N}(\text{C}_2\text{F}_5\text{SO}_2)_2]$, respectively, (see Figure 1, dashed lines) showing good agreement with the available data.

Figure 1. Density–temperature diagram of the $[\text{C}_2(\text{C}_6\text{F}_{13})\text{C}_1\text{Im}][\text{N}(\text{CF}_3\text{SO}_2)_2]$ and $[\text{C}_2(\text{C}_6\text{F}_{13})\text{C}_1\text{Im}][\text{N}(\text{C}_2\text{F}_5\text{SO}_2)_2]$ FILs. Experimental data (symbols) are taken from the literature.^{40,41} The solid lines represent soft-SAFT with optimized parameters obtained by fitting the *m* and ϵ molecular parameters, and the dashed lines were obtained by using soft-SAFT with transferred parameters from the $[\text{C}_{11}\text{C}_1\text{Im}][\text{N}(\text{CF}_3\text{SO}_2)_2]$ and $[\text{C}_{14}\text{C}_1\text{Im}][\text{N}(\text{CF}_3\text{SO}_2)_2]$ ⁶⁰ systems. See text for details.

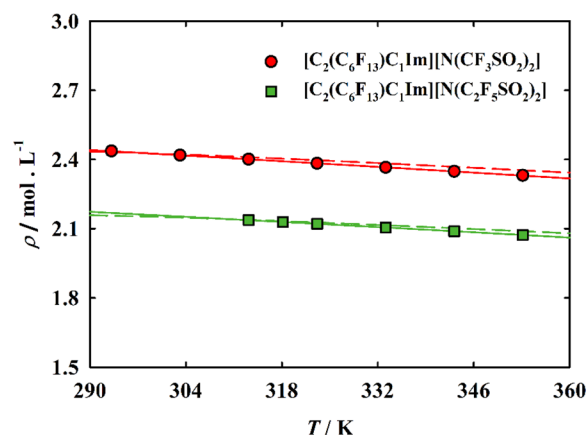


Figure 1. Density–temperature diagram of the $[\text{C}_2(\text{C}_6\text{F}_{13})\text{C}_1\text{Im}][\text{N}(\text{CF}_3\text{SO}_2)_2]$ and $[\text{C}_2(\text{C}_6\text{F}_{13})\text{C}_1\text{Im}][\text{N}(\text{C}_2\text{F}_5\text{SO}_2)_2]$ FILs. Experimental data (symbols) are taken from the literature.^{40,41} The solid lines represent soft-SAFT with optimized parameters obtained by fitting the *m* and ϵ molecular parameters, and the dashed lines were obtained by using soft-SAFT with transferred parameters from the $[\text{C}_{11}\text{C}_1\text{Im}][\text{N}(\text{CF}_3\text{SO}_2)_2]$ and $[\text{C}_{14}\text{C}_1\text{Im}][\text{N}(\text{CF}_3\text{SO}_2)_2]$ ⁶⁰ systems. See text for details.

With the aim to correct the differences of size/volume and energy between the $[\text{C}_2(\text{C}_6\text{F}_{13})\text{C}_1\text{Im}][\text{N}(\text{CF}_3\text{SO}_2)_2]$ and $[\text{C}_2(\text{C}_6\text{F}_{13})\text{C}_1\text{Im}][\text{N}(\text{C}_2\text{F}_5\text{SO}_2)_2]$ and the ILs of $[\text{C}_n\text{C}_1\text{Im}][\text{N}(\text{CF}_3\text{SO}_2)_2]$ series ($n = 11$ and 14), the association parameters and the molecular parameter σ were directly transferred from $[\text{C}_n\text{C}_1\text{Im}][\text{N}(\text{CF}_3\text{SO}_2)_2]$ series ($n = 11$ and 14) and fixed at the same value, whereas the parameters *m* and ϵ were adjusted to experimental data.^{40,41} These parameters are listed in Table 2, identified as $[\text{C}_2(\text{C}_6\text{F}_{13})\text{C}_1\text{Im}][\text{N}(\text{CF}_3\text{SO}_2)_2]$ and $[\text{C}_2(\text{C}_6\text{F}_{13})\text{C}_1\text{Im}][\text{N}(\text{C}_2\text{F}_5\text{SO}_2)_2]$ parameters. The density calculated with this new set of molecular parameters is in slightly better agreement with the experimental data as represented by the solid lines in Figure 1. The absolute average deviation (AAD) from density data, also provided in Table 2, is small in all cases.

In summary, molecular models of $[\text{C}_2(\text{C}_6\text{F}_{13})\text{C}_1\text{Im}][\text{N}(\text{CF}_3\text{SO}_2)_2]$ and $[\text{C}_2(\text{C}_6\text{F}_{13})\text{C}_1\text{Im}][\text{N}(\text{C}_2\text{F}_5\text{SO}_2)_2]$ FILs were proposed using transferable parameters and a holistic approach, by using the methodology previously established,²⁹ providing excellent agreement with available experimental data, further corroborating the robustness of the methodology. Once all soft-SAFT models are defined and parametrized, the next step is to study the solubility of F-gases in FILs, as discussed in the following section.

Solubility of Fluorinated Gases in Fluorinated Ionic Liquids. The selection of the systems for this study was based on the availability of experimental data from the literature, as well as the different molecular structures, in order to extract

information about the influence of the molecular structure in the solubility behavior.

As already mentioned, Sosa et al.⁴² studied the solubility of HFCs (R-32, R-125, and R-134a) in $[\text{C}_2\text{C}_1\text{Im}][\text{C}_4\text{F}_9\text{SO}_3]$, $[\text{C}_2\text{C}_1\text{Im}][\text{C}_4\text{F}_9\text{CO}_2]$, and $[\text{C}_2\text{C}_1\text{py}][\text{C}_4\text{F}_9\text{SO}_3]$. Soon after, Jovell et al.⁴⁴ used soft-SAFT EoS to assess the solubility of R134a in these three FILs. Lepre and co-workers determined experimentally the absorption of the HFC R-134a⁴¹ and of the perfluoroalkanes R-14, R-116, and R-218⁴⁰ in $[\text{C}_2(\text{C}_6\text{F}_{13})\text{-C}_1\text{Im}][\text{N}(\text{CF}_3\text{SO}_2)_2]$ and $[\text{C}_2(\text{C}_6\text{F}_{13})\text{C}_1\text{Im}][\text{N}(\text{C}_2\text{F}_5\text{SO}_2)_2]$.

In this work, we assess the ability of soft-SAFT to predict the solubility of the F-gases in these ILs. Therefore, to study the solubilities of R-32 and R-125 in $[\text{C}_2\text{C}_1\text{Im}][\text{C}_4\text{F}_9\text{SO}_3]$, $[\text{C}_2\text{C}_1\text{Im}][\text{C}_4\text{F}_9\text{CO}_2]$, and $[\text{C}_2\text{C}_1\text{py}][\text{C}_4\text{F}_9\text{SO}_3]$, for consistency, we have used the same approach previously done for R-134a solubility in these FILs.⁴⁴ Given the nonideality of the mixtures, two binary parameters were needed to accurately reproduce the experimental data. The η parameter (eq 2), taking into account the different volumes of the groups, was transferred from the study of the solubility of R-134a in the selected ILs,⁴⁴ fixed to 1.049, while the ξ energy parameter (eq 3) was fitted for each F-gas/ILs pair to have the best representation of the experimental data (see Table 3). Notice that for $[\text{C}_2(\text{C}_6\text{F}_{13})\text{C}_1\text{Im}][\text{N}(\text{CF}_3\text{SO}_2)_2]$ and $[\text{C}_2(\text{C}_6\text{F}_{13})\text{-C}_1\text{Im}][\text{N}(\text{C}_2\text{F}_5\text{SO}_2)_2]$ only one binary parameter (ξ) was needed for all the studied gases, keeping η equal to one (see Table 3). For the case of HFCs with FILs, best results were obtained with values of the binary energy parameter greater

than one, except for R-134a. The opposite behavior was found for perfluoroalkanes, with values of ξ smaller than 1. These results revealed that the interaction of the HFCs, polar fluids, with the FILs is stronger than those of the pure fluids, whereas, for the perfluoroalkanes, the opposite is found. This behavior was previous observed when studying the solubility of F-gases and other gases in ILs.^{44,50,51} Notice that not specific interactions, other than the Lorentz–Berthelot mixing rules for the LJ monomers (eqs 2 and 3) and the calculated average of the cross-association between the HFCs and the FILs (eqs 4 and 5), have been considered in the mixtures, which may be too simple for the complex interactions existing between the HFCs and perfluoroalkanes with the FILs.

The solubilities of R-32 and R-125 in $[\text{C}_2\text{C}_1\text{Im}][\text{C}_4\text{F}_9\text{SO}_3]$, $[\text{C}_2\text{C}_1\text{Im}][\text{C}_4\text{F}_9\text{CO}_2]$, and $[\text{C}_2\text{C}_1\text{py}][\text{C}_4\text{F}_9\text{SO}_3]$ were calculated at 303.15 K, and results can be found in Figure 2, compared to those of R-134a absorption in the same FILs from ref 44 for comparative purposes. As inferred from the figure, soft-SAFT calculations for all HFCs are very accurate compared to experimental data. It was also observed that the three FILs have a similar ability to absorb the R-32, R-125, and R-134a in the studied range of pressures, inferring that the leading molecular interactions are similar in all cases.

The solubility of R-134a in $[\text{C}_2(\text{C}_6\text{F}_{13})\text{C}_1\text{Im}][\text{N}(\text{CF}_3\text{SO}_2)_2]$ and in $[\text{C}_2(\text{C}_6\text{F}_{13})\text{C}_1\text{Im}][\text{N}(\text{C}_2\text{F}_5\text{SO}_2)_2]$ FILs, obtained by soft-SAFT and compared to experimental results, is illustrated in Figure 3. The ξ parameter was adjusted to the intermediate temperature (323.15 K) and used to predict the solubilities at 303.15 and 343.15 K. For both FILs, a good agreement was found for all the studied temperatures, showing the robustness of the soft-SAFT model. As expected, the increment of temperature impairs the solubility of R-134a in both FILs, while when comparing both FILs, the increment of the fluorine content in the anion does not significantly affect the solubility of R-134a, having similar behavior.

Finally, Figure 4 shows the absorption of the linear perfluoroalkanes (R-14, R-116, and R-218) in the FILs $[\text{C}_2(\text{C}_6\text{F}_{13})\text{C}_1\text{Im}][\text{N}(\text{CF}_3\text{SO}_2)_2]$ and $[\text{C}_2(\text{C}_6\text{F}_{13})\text{C}_1\text{Im}][\text{N}(\text{C}_2\text{F}_5\text{SO}_2)_2]$ at 0.07 MPa, with soft-SAFT calculations showing good agreement with experimental data by using a ξ parameter for each F-gas/IL pair (see Table 3). It is observed that both FILs have the same ability to solubilize the studied gases, increasing in the following order: R-14 < R-116 < R-218. Higher temperatures also decrease the solubilities of these gases, which is more pronounced in the case of R-218.

Influence of the Structural Features of Fluorinated Ionic Liquids in the Absorption of Fluorinated Gases.

Once the model and parameters of FILs and F-gases are obtained and validated with experimental data, they can be used to predict the properties of these systems at other thermodynamic conditions (e.g., pressure and temperature) in a reliable manner, as they do not depend on the conditions at which they were fitted. In this way, it is possible to obtain relevant information on how the structural features of these complex systems can affect the absorption performance and highlight the best characteristics of FILs that favor the solubility of F-gases. With this aim in mind, the diagrams of solubility of the six F-gases in the five FILs were calculated using soft-SAFT with two different approaches: (i) varying the temperature in the range of 300 to 400 K and at constant atmospheric pressure (see Figure 5) and (ii) changing the pressure between 0 and 3 MPa, at the constant temperatures of 343.15 and 303.15 K (Figure 6). Please, notice that the goal of

Table 3. Binary Energy Interaction Parameter Values, ξ and η , for Binary Mixtures of F-Gases with FILs

FILs	F-gas	ξ	η	ref
$[\text{C}_2\text{C}_1\text{Im}][\text{C}_4\text{F}_9\text{CO}_2]$	R-32 (CH_2F_2)	1.141	1.049	this work
	R-125 (C_2HF_5)	1.234	1.049	this work
	R-134a ($\text{C}_2\text{H}_2\text{F}_4$)	1.146	1.049	44
$[\text{C}_2\text{C}_1\text{Im}][\text{C}_4\text{F}_9\text{SO}_3]$	R-32 (CH_2F_2)	1.141	1.049	this work
	R-125 (C_2HF_5)	1.214	1.049	this work
	R-134a ($\text{C}_2\text{H}_2\text{F}_4$)	1.140	1.049	44
$[\text{C}_2\text{C}_1\text{py}][\text{C}_4\text{F}_9\text{SO}_3]$	R-32 (CH_2F_2)	1.161	1.049	this work
	R-125 (C_2HF_5)	1.238	1.049	this work
	R-134a ($\text{C}_2\text{H}_2\text{F}_4$)	1.157	1.049	44
$[\text{C}_2(\text{C}_6\text{F}_{13})\text{C}_1\text{Im}][\text{N}(\text{CF}_3\text{SO}_2)_2]$	R-134a ($\text{C}_2\text{H}_2\text{F}_4$)	1.060	1.000	this work
	R-14 (CF_4)	0.850	1.000	this work
	R-116 (C_2F_6)	0.900	1.000	this work
	R-218 (C_3F_8)	0.930	1.000	this work
$[\text{C}_2(\text{C}_6\text{F}_{13})\text{C}_1\text{Im}][\text{N}(\text{C}_2\text{F}_5\text{SO}_2)_2]$	R-134a ($\text{C}_2\text{H}_2\text{F}_4$)	1.040	1.000	this work
	R-14 (CF_4)	0.830	1.000	this work
	R-116 (C_2F_6)	0.890	1.000	this work
	R-218 (C_3F_8)	0.930	1.000	this work

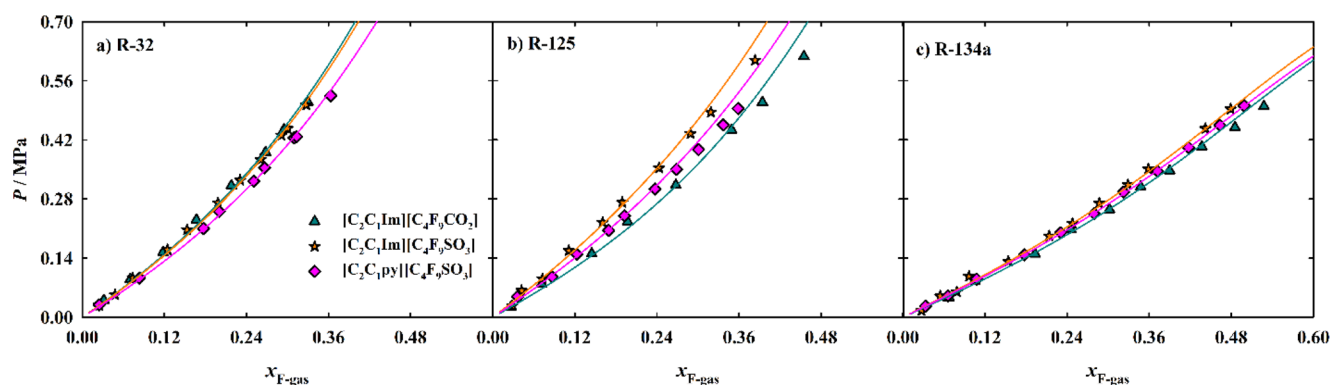


Figure 2. Solubility of (a) R-32, (b) R-125, and (c) R-134a gases in $[\text{C}_2\text{C}_1\text{Im}][\text{C}_4\text{F}_9\text{SO}_3]$, $[\text{C}_2\text{C}_1\text{Im}][\text{C}_4\text{F}_9\text{CO}_2]$, and $[\text{C}_2\text{C}_1\text{py}][\text{C}_4\text{F}_9\text{SO}_3]$. The symbols represent the experimental data,⁴² and the lines represent the soft-SAFT calculations. The calculations in panel c are from the literature,⁴⁴ and are shown here for comparative purposes.

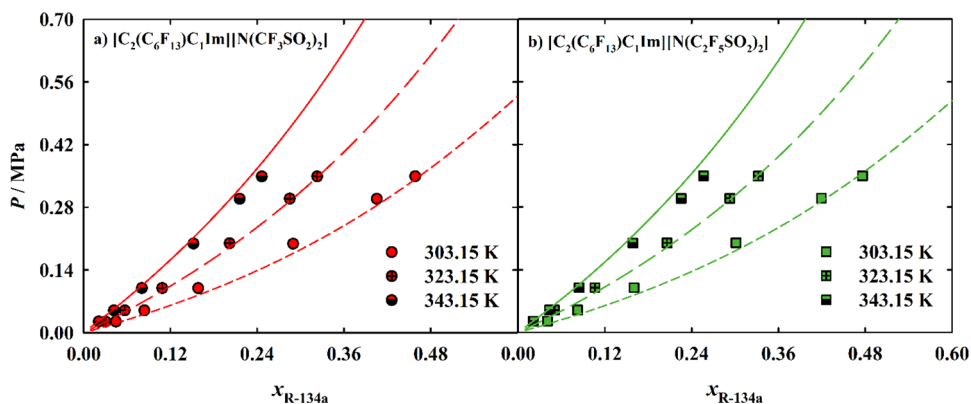


Figure 3. Solubility of R-134a in $[\text{C}_2(\text{C}_6\text{F}_{13})\text{C}_1\text{Im}][\text{N}(\text{CF}_3\text{SO}_2)_2]$ and $[\text{C}_2(\text{C}_6\text{F}_{13})\text{C}_1\text{Im}][\text{N}(\text{C}_2\text{F}_5\text{SO}_2)_2]$. Symbols represent the experimental data,⁴¹ and lines represent the soft-SAFT calculations.

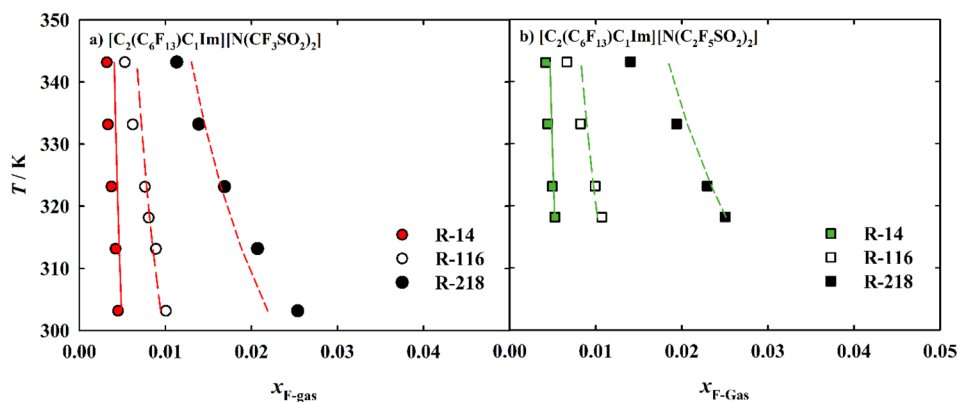


Figure 4. Solubility of R-14, R-116, and R-128 in $[\text{C}_2(\text{C}_6\text{F}_{13})\text{C}_1\text{Im}][\text{N}(\text{CF}_3\text{SO}_2)_2]$ and $[\text{C}_2(\text{C}_6\text{F}_{13})\text{C}_1\text{Im}][\text{N}(\text{C}_2\text{F}_5\text{SO}_2)_2]$. The symbols represent the experimental data⁴⁰ and the lines are the soft-SAFT calculations from this work.

these calculations is not to provide quantitative predictions (as there is not experimental data available for some of these systems to compare to), but to explore the trends for all cases following the same approach; in order to do this, the binary parameters (ξ and η) were set to unity in all cases.

Results presented in Figure 5 show that the decrease of temperature favors the absorption of all gases by the FILs, as expected. This behavior is more pronounced in the systems with $[\text{C}_2(\text{C}_6\text{F}_{13})\text{C}_1\text{Im}][\text{N}(\text{CF}_3\text{SO}_2)_2]$ and $[\text{C}_2(\text{C}_6\text{F}_{13})\text{C}_1\text{Im}][\text{N}(\text{C}_2\text{F}_5\text{SO}_2)_2]$ FILs. The absorption of the six F-gases in $[\text{C}_2\text{C}_1\text{Im}][\text{C}_4\text{F}_9\text{SO}_3]$, $[\text{C}_2\text{C}_1\text{Im}][\text{C}_4\text{F}_9\text{CO}_2]$, and $[\text{C}_2\text{C}_1\text{py}][\text{C}_4\text{F}_9\text{SO}_3]$

is very similar when compared to each other. Only a minor decrease of solubility of R-32, R-125, and R-134a is found for $[\text{C}_2\text{C}_1\text{py}][\text{C}_4\text{F}_9\text{SO}_3]$, indicating that the imidazolium cation has better absorption power (see Figure 5a–c). No significant difference is found when comparing the functional group of $[\text{C}_4\text{F}_9\text{SO}_3]^-$ and $[\text{C}_4\text{F}_9\text{CO}_2]^-$ anions. Some higher values are found for the case of R-32 and R-134a absorption in these three FILs (Figure 5a,c) when compared to the remaining F-gases. The solubility of the F-gases in the $[\text{C}_2\text{C}_1\text{Im}][\text{C}_4\text{F}_9\text{SO}_3]$, $[\text{C}_2\text{C}_1\text{Im}][\text{C}_4\text{F}_9\text{CO}_2]$, and $[\text{C}_2\text{C}_1\text{py}][\text{C}_4\text{F}_9\text{SO}_3]$ FILs is significantly lower than the values found

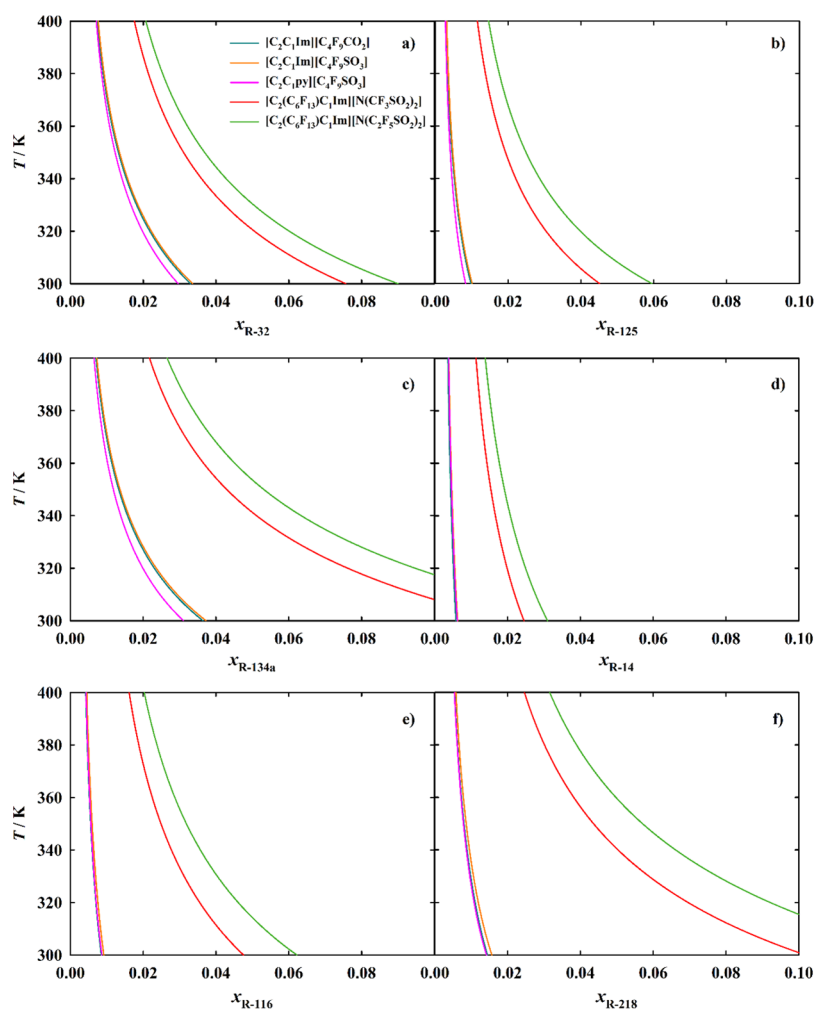


Figure 5. Effect of the temperature, predicted by soft-SAFT, in the absorption of (a) R-32, (b) R-125, (c) R-134a, (d) R-14, (e) R-116, and (f) R-218 in $[\text{C}_2\text{C}_1\text{Im}][\text{C}_4\text{F}_9\text{SO}_3]$ (cyan), $[\text{C}_2\text{C}_1\text{Im}][\text{C}_4\text{F}_9\text{CO}_2]$ (orange), $[\text{C}_2\text{C}_1\text{py}][\text{C}_4\text{F}_9\text{SO}_3]$ (pink), $[\text{C}_2(\text{C}_6\text{F}_{13})\text{C}_1\text{Im}][\text{N}(\text{CF}_3\text{SO}_2)_2]$ (red), and $[\text{C}_2(\text{C}_6\text{F}_{13})\text{C}_1\text{Im}][\text{N}(\text{C}_2\text{F}_5\text{SO}_2)_2]$ (green) at atmospheric pressure.

for $[\text{C}_2(\text{C}_6\text{F}_{13})\text{C}_1\text{Im}][\text{N}(\text{CF}_3\text{SO}_2)_2]$ and $[\text{C}_2(\text{C}_6\text{F}_{13})\text{C}_1\text{Im}][\text{N}(\text{C}_2\text{F}_5\text{SO}_2)_2]$. This behavior indicates that the presence of a perfluoroalkyl chain in the imidazolium cation and the bulkier anion favors the absorption of these gases when compared with FILs that have anionic and linear perfluoroalkyl chains. Moreover, in all cases, the $[\text{C}_2(\text{C}_6\text{F}_{13})\text{C}_1\text{Im}][\text{N}(\text{C}_2\text{F}_5\text{SO}_2)_2]$ shows a superior solubility of F-gases than the $[\text{C}_2(\text{C}_6\text{F}_{13})\text{C}_1\text{Im}][\text{N}(\text{CF}_3\text{SO}_2)_2]$, indicating that the addition of one carbon to the two anionic symmetric fluorinated chains also contributes to the gas-philicity of the FILs. Both $[\text{C}_2(\text{C}_6\text{F}_{13})\text{C}_1\text{Im}][\text{N}(\text{CF}_3\text{SO}_2)_2]$ and $[\text{C}_2(\text{C}_6\text{F}_{13})\text{C}_1\text{Im}][\text{N}(\text{C}_2\text{F}_5\text{SO}_2)_2]$ have a higher level of absorption of gases having more fluorine atoms. This is seen for HFCs, for which the gas absorption has the tendency: R-32 < R-125 < R-134a; and for PFCs for which R-14 < R-116 < R-218.

Figure 6 depicts the influence of the pressure, keeping the temperature constant. In this case, the calculations were executed at two different temperatures, which also gives information on the temperature effect. Results show that the increase of temperature decreases the solubility of F-gases in the FILs, as expected. However, the increase of pressure has the opposite effect, benefiting the absorption of all gases. When comparing all the systems at the same temperature, very similar conclusions can be extracted. The $[\text{C}_2\text{C}_1\text{Im}][\text{C}_4\text{F}_9\text{SO}_3]$,

$[\text{C}_2\text{C}_1\text{Im}][\text{C}_4\text{F}_9\text{CO}_2]$, and $[\text{C}_2\text{C}_1\text{py}][\text{C}_4\text{F}_9\text{SO}_3]$ have a quite similar behavior for all systems. In the case of R-32, R-125, and R-134a a more pronounced reduction of gas solubility for the $[\text{C}_2\text{C}_1\text{py}][\text{C}_4\text{F}_9\text{SO}_3]$ is found (Figure 6a–c). The FILs based on bulkier anions and the imidazolium cation with a perfluoroalkyl side chain have a higher intake of absorbed F-gases compared to the ones based on anionic perfluoroalkyl chains. The increment of one carbon atom from $[\text{C}_2(\text{C}_6\text{F}_{13})\text{C}_1\text{Im}][\text{N}(\text{CF}_3\text{SO}_2)_2]$ to $[\text{C}_2(\text{C}_6\text{F}_{13})\text{C}_1\text{Im}][\text{N}(\text{C}_2\text{F}_5\text{SO}_2)_2]$ increases the absorption of all studied F-gases. As long as the number of fluorine atoms increases in the structure of the F-gases, the absorption in the $[\text{C}_2(\text{C}_6\text{F}_{13})\text{C}_1\text{Im}][\text{N}(\text{CF}_3\text{SO}_2)_2]$ and $[\text{C}_2(\text{C}_6\text{F}_{13})\text{C}_1\text{Im}][\text{N}(\text{C}_2\text{F}_5\text{SO}_2)_2]$ also increases.

Therefore, from the results obtained in this work, the ideal FIL for solubilizing F-gas should be designed preferably with an imidazolium cation, and the solubility is promoted if it is functionalized with a perfluoroalkyl side chain. The bulkier anions based on the $[\text{N}(\text{C}_m\text{F}_{2m+1}\text{SO}_2)_2]^-$ series have better performance to absorb the studied gases. Finally, the amount of fluorine atoms on the gas also increases their absorption by FILs, another characteristic that must be accounted for when choosing the best structural characteristics of FILs to be used in capturing and recovering F-gases from air conditioning, refrigeration, and heat equipment systems.

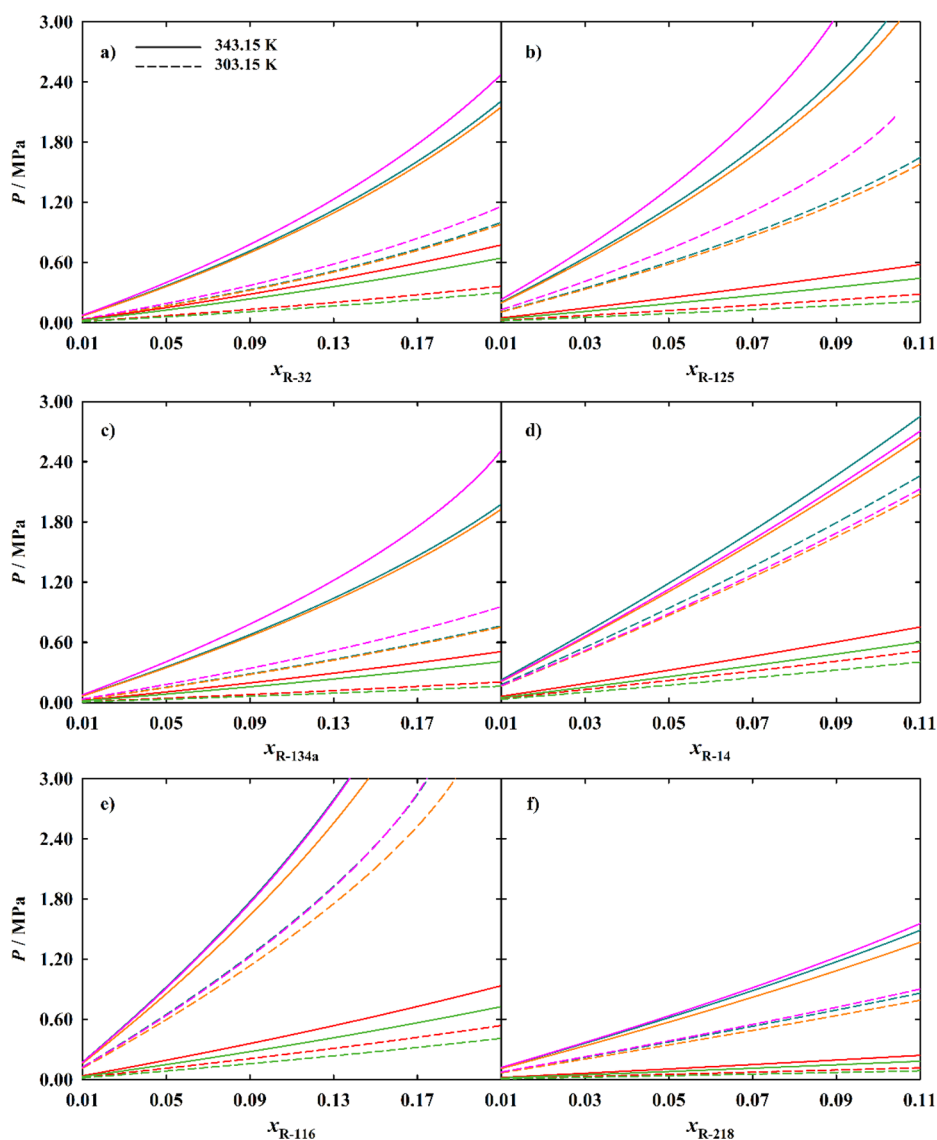


Figure 6. Effect of the pressure, predicted by soft-SAFT, in the absorption of (a) R-32, (b) R-125, (c) R-134a, (d) R-14, (e) R-116, and (f) R-218 in $[\text{C}_2\text{C}_1\text{Im}][\text{C}_4\text{F}_9\text{SO}_3]$ (cyan), $[\text{C}_2\text{C}_1\text{Im}][\text{C}_4\text{F}_9\text{CO}_2]$ (orange), $[\text{C}_2\text{C}_1\text{py}][\text{C}_4\text{F}_9\text{SO}_3]$ (pink), $[\text{C}_2(\text{C}_6\text{F}_{13})\text{C}_1\text{Im}][\text{N}(\text{CF}_3\text{SO}_2)_2]$ (red), and $[\text{C}_2(\text{C}_6\text{F}_{13})\text{C}_1\text{Im}][\text{N}(\text{C}_2\text{F}_5\text{SO}_2)_2]$ (green) at two different temperatures (solid lines, 343.15 K; short dashed lines, 303.15 K).

To further assess the solubility of the F-gases in the FILs, additional thermodynamic properties/parameters were considered and determined in the work, such as Henry constants, enthalpy and entropy of dissolution, and the Hildebrand solubility parameter. Henry's constants were calculated using eq 8, which suggests that a smaller value of H_C corresponds to a larger absorption of F-gas by the FIL. The values of H_C for each FIL + F-gas system are provided in Table 4. Results are consistent with the trends found for the studied solubility diagrams. The H_C values are lower for the lower temperature, indicating higher solubility of F-gas. In this sense, lower values of H_C were found to $[\text{C}_2(\text{C}_6\text{F}_{13})\text{C}_1\text{Im}][\text{N}(\text{CF}_3\text{SO}_2)_2]$ and $[\text{C}_2(\text{C}_6\text{F}_{13})\text{C}_1\text{Im}][\text{N}(\text{C}_2\text{F}_5\text{SO}_2)_2]$ FILs for all F-gases, compared to the higher values obtained to the FILs with linear fluorinated anions and without fluorination in the cation. All FILs show a similar tendency to absorb the studied F-gases, which is $\text{R-14} < \text{R-116} \approx \text{R-125} < \text{R-218} < \text{R-32} \approx \text{R-134a}$. Therefore, results indicate that there is not a direct correlation between the fluorine content and the structure of the F-gases

with the FILs ability to absorb them, and case by case studies should be performed for each system.

The enthalpy ($\Delta_{\text{dis}}H$) and entropy ($\Delta_{\text{dis}}S$) of dissolution were also considered in this work to obtain information on the strength of the interactions and the degree of order of the F-gases dissolved in the FILs, respectively.^{57,74} These two thermodynamic parameters were calculated by eqs 9 and 10 with the values of H_C previously determined at low gas compositions. Values of $\Delta_{\text{dis}}H$ and $\Delta_{\text{dis}}S$ for each F-gas + FIL system are provided in Table 4. Results indicate that for $[\text{C}_2\text{C}_1\text{Im}][\text{C}_4\text{F}_9\text{SO}_3]$, $[\text{C}_2\text{C}_1\text{Im}][\text{C}_4\text{F}_9\text{CO}_2]$, and $[\text{C}_2\text{C}_1\text{py}][\text{C}_4\text{F}_9\text{SO}_3]$, the enthalpy and entropy values become more negative, in the order $\text{R-14} < \text{R-116} < \text{R-218} < \text{R-125} < \text{R-32} < \text{R-134a}$, whereas for $[\text{C}_2(\text{C}_6\text{F}_{13})\text{C}_1\text{Im}][\text{N}(\text{CF}_3\text{SO}_2)_2]$ and $[\text{C}_2(\text{C}_6\text{F}_{13})\text{C}_1\text{Im}][\text{N}(\text{C}_2\text{F}_5\text{SO}_2)_2]$ the order is $\text{R-14} < \text{R-116} < \text{R-218} \approx \text{R-125} < \text{R-32} < \text{R-134a}$. A negative enthalpy and a positive entropy favor the dissolution of the F-gas in the FIL. This means that for all cases, R134a has a higher energy of interaction with all the FILs, increasing the absorption of this gas. However, the negative entropy might indicate a

Table 4. Henry Constants (H_C) Determined at 303.15 and 343.15 K, and Enthalpy ($\Delta_{\text{dis}}H$) and Entropy ($\Delta_{\text{dis}}S$) of Dissolution Calculated from the Henry Constants for the Binary Mixtures of F-Gases with the FILs

FILs	F-gas	H_C (MPa)		$\Delta_{\text{dis}}H$	$\Delta_{\text{dis}}S$
		343.15 K	303.15 K	(kJ/mol)	(J/mol K)
[C ₂ C ₁ Im][C ₄ F ₉ CO ₂]	R-32	7.49	3.46	-16.7	-51.8
	R-125	23.5	12.3	-14.0	-43.4
	R-134a	7.20	3.08	-18.4	-57.0
	R-14	24.1	19.1	-5.0	-15.6
	R-116	18.7	13.1	-7.7	-23.9
	R-218	12.5	7.52	-11.0	-34.1
[C ₂ C ₁ Im][C ₄ F ₉ SO ₃]	R-32	7.31	3.39	-16.6	-51.5
	R-125	22.6	11.9	-13.9	-43.0
	R-134a	7.02	3.01	-18.3	-56.8
	R-14	22.4	17.6	-5.2	-16.2
	R-116	17.3	12.1	-7.7	-24.0
	R-218	11.6	6.94	-11.1	-34.5
[C ₂ C ₁ py][C ₄ F ₉ SO ₃]	R-32	8.14	3.88	-16.0	-49.7
	R-125	27.5	15.0	-13.1	-40.7
	R-134a	8.25	3.65	-17.6	-54.7
	R-14	22.8	17.9	-5.2	-16.2
	R-116	18.5	12.9	-7.8	-24.2
	R-218	12.8	7.76	-10.8	-33.6
[C ₂ (C ₆ F ₁₃)C ₁ Im][N(CF ₃ SO ₂) ₂]	R-32	3.04	1.41	-16.6	-51.5
	R-125	4.98	2.44	-15.4	-47.9
	R-134a	2.12	0.86	-19.5	-60.5
	R-14	6.50	4.43	-8.3	-25.7
	R-116	3.88	2.26	-11.7	-36.3
	R-218	2.12	1.04	-15.4	-47.8
[C ₂ (C ₆ F ₁₃)C ₁ Im][N(C ₂ F ₅ SO ₂) ₂]	R-32	2.54	1.17	-16.8	-52.0
	R-125	3.82	1.83	-15.9	-49.4
	R-134a	1.69	0.67	-20.0	-62.1
	R-14	5.20	3.49	-8.6	-26.8
	R-116	3.01	1.71	-12.2	-37.9
	R-218	1.60	0.77	-15.8	-49.1

condensation of the gas, and this behavior was also found in the study of F-gases with other ILs.⁵⁷ The comparison between FILs shows that [C₂(C₆F₁₃)C₁Im][N(CF₃SO₂)₂] and [C₂(C₆F₁₃)C₁Im][N(C₂F₅SO₂)₂] have more negative values of enthalpy for almost all gases (except R-32 where similar values were obtained for all FILs) compared to [C₂C₁Im]-[C₄F₉SO₃], [C₂C₁Im][C₄F₉CO₂], and [C₂C₁py][C₄F₉SO₃], supporting the results previously discussed.

Finally, the solubility parameters of FILs and F-gases calculated from eq 11⁷⁵ are provided in Table 5. It is observed that [C₂C₁Im][C₄F₉CO₂], [C₂C₁Im][C₄F₉SO₃], and [C₂C₁py][C₄F₉SO₃] have very similar values of δ , as it happens for [C₂(C₆F₁₃)C₁Im][N(CF₃SO₂)₂] and [C₂(C₆F₁₃)-C₁Im][N(C₂F₅SO₂)₂]. Regarding the F-gases, different values are obtained for each of them, with the HFCs showing greater

values than the perfluoroalkanes, in general, as a consequence their polar nature, and hence, higher cohesive energy density.

In principle, a solvent has more ability to solubilize a solute that has a similar value of δ . According to the results presented in Table 5, the [C₂C₁Im][C₄F₉SO₃], [C₂C₁Im][C₄F₉CO₂], and [C₂C₁py][C₄F₉SO₃] FILs have closer values of δ than [C₂(C₆F₁₃)C₁Im][N(CF₃SO₂)₂] and [C₂(C₆F₁₃)C₁Im][N-(C₂F₅SO₂)₂] for almost F-gases, except R-14. This should indicate that they have more ability to solubilize these gases. However, as demonstrated by the results discussed earlier in this contribution, the best FILs to solubilize the F-gases are [C₂(C₆F₁₃)C₁Im][N(CF₃SO₂)₂] and [C₂(C₆F₁₃)C₁Im][N-(C₂F₅SO₂)₂]. Notice that the Hildebrand parameter is related to the cohesive energy of the pure fluids, and it is known to be accurate for nonpolar solvents; hence, for the systems investigated in this work, having similar Hildebrand parameters does not necessarily lead to good solubility power, pinpointing the high complexity of the interactions occurring between the F-gases and FILs, and the polar nature of them.

Table 5. Hildebrand Solubility Parameter (δ) Determined to Each FIL and F-Gas at 343.15 K

FIL	δ (MPa ^{0.5})	F-gas	δ (MPa ^{0.5})
[C ₂ C ₁ Im][C ₄ F ₉ CO ₂]	23.59	R-32	25.85
[C ₂ C ₁ Im][C ₄ F ₉ SO ₃]	23.23	R-125	25.63
[C ₂ C ₁ py][C ₄ F ₉ SO ₃]	23.30	R-134a	27.88
[C ₂ (C ₆ F ₁₃)C ₁ Im][N(CF ₃ SO ₂) ₂]	17.51	R-14	18.41
[C ₂ (C ₆ F ₁₃)C ₁ Im][N(C ₂ F ₅ SO ₂) ₂]	17.58	R-116	22.31
		R-218	25.00

CONCLUSIONS

Soft-SAFT EoS was used in this work to showcase the absorption behavior of F-gases in FILs. Five different FILs ([C₂C₁Im][C₄F₉SO₃], [C₂C₁Im][C₄F₉CO₂], [C₂C₁py]-[C₄F₉SO₃], [C₂(C₆F₁₃)C₁Im][N(CF₃SO₂)₂], and [C₂(C₆F₁₃)-C₁Im][N(C₂F₅SO₂)₂]), three PFCs (R-14, R-116, and R-218) and three HFCs (R-32, R-125, and R-134a) were chosen for

this purpose. To achieve that goal, $[\text{C}_2(\text{C}_6\text{F}_{13})\text{C}_1\text{Im}][\text{N}(\text{CF}_3\text{SO}_2)_2]$ and $[\text{C}_2(\text{C}_6\text{F}_{13})\text{C}_1\text{Im}][\text{N}(\text{C}_2\text{F}_5\text{SO}_2)_2]$ were modeled using soft-SAFT for the first time in this work. The molecular models accurately predict the density of both FILs, evidencing once again the strength of soft-SAFT to modeling FILs in a simple and fast manner.

The solubility of the F-gases in these FILs was successfully captured by soft-SAFT in all cases. The $[\text{C}_2\text{C}_1\text{Im}][\text{C}_4\text{F}_9\text{SO}_3]$, $[\text{C}_2\text{C}_1\text{Im}][\text{C}_4\text{F}_9\text{CO}_2]$, and $[\text{C}_2\text{C}_1\text{py}][\text{C}_4\text{F}_9\text{SO}_3]$ and F-gases have more complex interactions, and two binary parameters were needed for a quantitative agreement of the experimental solubility, whereas for $[\text{C}_2(\text{C}_6\text{F}_{13})\text{C}_1\text{Im}][\text{N}(\text{CF}_3\text{SO}_2)_2]$ and $[\text{C}_2(\text{C}_6\text{F}_{13})\text{C}_1\text{Im}][\text{N}(\text{C}_2\text{F}_5\text{SO}_2)_2]$, only the energy binary parameter was fitted. Once the parametrization of all systems was concluded, soft-SAFT was used in a systematic manner to extract trends on the influence of the molecular structure of the FILs and F-gases on their absorption behavior. For this purpose, the solubility of the six F-gases in the five studied FILs was calculated using soft-SAFT exactly at the same thermodynamic conditions. Moreover, the values of thermodynamic parameters such as Henry constants, enthalpy and entropy of dissolution, and Hildebrand constants were determined with soft-SAFT EoS. As expected, the increment of temperature reduces the absorption of gases, whereas the opposite behavior is found when increasing the pressure. The FILs with bulkier anions and the perfluoroalkyl side chains in the imidazolium cations showed a higher degree of absorption of all gases, with better results for the F-gases with a higher number of fluorine atoms in their structure. Hence, the interactions between FILs and F-gases fluorinated counterparts play a critical role in the solubility mechanisms as well as the amount of fluorine content in the structure of both systems.

Among the systems studied in this work, $[\text{C}_2(\text{C}_6\text{F}_{13})\text{C}_1\text{Im}][\text{N}(\text{C}_2\text{F}_5\text{SO}_2)_2]$ is the most promising FIL for capturing and separating F-gases. However, understanding the solubility is only a first step toward finding the best FILs; other properties of the FILs must be considered to ensure a higher solubility of F-gases. For instance, the addition of carbon atoms in the perfluoroalkyl chains of FILs not only increases the viscosity but also results in more toxic compounds, which can hinder their application in this field. Therefore, a balance must be found between the absorption of F-gases, viscosity, and toxicity obtained when adding a higher number of fluorinated counterparts in the FILs structure, before proceeding to the application of these new systems in the capture and recovery of F-gases. With this in mind, $[\text{C}_2(\text{C}_6\text{F}_{13})\text{C}_1\text{Im}][\text{N}(\text{CF}_3\text{SO}_2)_2]$ seems an excellent candidate, as it shows a significant absorption performance for all gases while being environmentally friendlier than the other FILs. This work also highlights the need of using robust models as a screening tool to assess different solvents for this application, before embarking on long experimental studies, which can be performed guided by these approaches, hastening the process of moving the FILs from the laboratory to industrial implementation.

AUTHOR INFORMATION

Corresponding Authors

Ana B. Pereiro – LAQV, REQUIMTE, Department of Chemistry, NOVA School of Science and Technology, NOVA University Lisbon, Caparica 2829-516, Portugal;
orcid.org/0000-0001-7166-6764; Email: anab@fct.unl.pt

Lourdes F. Vega – Research and Innovation Center on CO₂ and Hydrogen (RICH Center) and Chemical Engineering Department, Khalifa University, Abu Dhabi, United Arab Emirates; orcid.org/0000-0002-7609-4184;
Email: lourdes.vega@ku.ac.ae

Authors

Margarida L. Ferreira – LAQV, REQUIMTE, Department of Chemistry, NOVA School of Science and Technology, NOVA University Lisbon, Caparica 2829-516, Portugal;
orcid.org/0000-0002-8119-3881
João M. M. Araújo – LAQV, REQUIMTE, Department of Chemistry, NOVA School of Science and Technology, NOVA University Lisbon, Caparica 2829-516, Portugal;
orcid.org/0000-0002-8648-7539

Complete contact information is available at:
<https://pubs.acs.org/10.1021/acs.jced.1c00984>

Author Contributions

M.L.F. performed the detailed calculations. The manuscript was written through contributions of all authors. All authors have given approval to the final version of the manuscript.

Notes

The authors declare no competing financial interest.

ACKNOWLEDGMENTS

This work is dedicated to Professor Joan Brennecke, for her outstanding contributions in the field of ionic liquids and for successfully leading the *Journal of Chemical Engineering Data* all these years. Special thanks from Prof. Vega, for all these years of very fruitful scientific conversations and for your friendship. Several useful discussions with Dr. Ismail Alkhatib are gratefully acknowledged. The authors would like to acknowledge the financial support from FCT/MCTES (Portugal), through Grants SFRH/BD/130965/2017 and COVID/BD/151919/2021 (M.L.F.), contracts 2020.00835.CEEIND (J.M.M.A.) and 2021.01432.CEECIND (A.B.P.), and project PTDC/EQU-EQU/29737/2017. This work was also supported by the Associate Laboratory for Green Chemistry—LAQV which is financed by national funds from FCT/MCTES (UIDB/50006/2020). Additional financial support has been provided by Khalifa University of Science and Technology through project RC2-2019-007. Computational resources from the Research and Innovation Center on CO₂ and Hydrogen (RICH Center) and from the Almesbar HPC at Khalifa University are gratefully acknowledged.

REFERENCES

- (1) United Nations. Climate Action. *What is climate change?* <https://www.un.org/en/climatechange/what-is-climate-change> (accessed 2021-11-12).
- (2) United Nations Environment Programme (2021). *Emissions Gap Report 2021: The Heat Is On – A World of Climate Promises Not Yet Delivered*. Nairobi <https://www.unep.org/resources/emissions-gap-report-2021> (accessed 2021-11-12).
- (3) IPCC. *Summary for Policymakers*. In: *Climate Change 2021: The Physical Science Basis. Contribution of Working Group I to the Sixth Assessment Report of the Intergovernmental Panel on Climate Change* Masson-Delmotte, V., Zhai, P., Pirani, A., Connors, S.L.; Péan, C., Berger, S., Caud, N., Chen, Y., Goldfarb, L., Gomis, M.I., Huang, M., Leitzell, K., Lonnoy, E.; Matthews, J.B.R., Maycock, T.K., Waterfield, T., Yelekçi, O., Yu, R., Zhou, B., Eds.; Cambridge University Press. 2022; in press.

- (4) European Commission. *Fluorinated greenhouse gases*. https://ec.europa.eu/clima/eu-action/fluorinated-greenhouse-gases_en (accessed 2021–11–12).
- (5) United States Environmental Protection Agency. *Greenhouse Gas Emissions. Overview of Greenhouse Gases*. <https://www.epa.gov/ghemissions/overview-greenhouse-gases> (accessed 2021–11–12).
- (6) Calm, J. M. The next generation of refrigerants - Historical review, considerations, and outlook. *Int. J. Refrig.* **2008**, *31* (7), 1123–1133.
- (7) United Nations. *Handbook for the Montreal Protocol on Substances that Deplete the Ozone Layer, 9th ed.*; Ozone Secretariat, U.N.: 2012.
- (8) United Nations. Climate change. *What is the Kyoto protocol?* https://unfccc.int/kyoto_protocol (accessed 2021–11–12).
- (9) Heath, E. A. Amendment to the Montreal Protocol on Substances that Deplete the Ozone Layer (Kigali Amendment). *Int. Leg. Mater.* **2017**, *56* (1), 193–205.
- (10) European Union. *Regulation (EU) No 517/2014 of the European Parliament and of the Council of 16 April 2014 on Fluorinated Greenhouse Gases and Repealing Regulation (EC) No 842/2006*; European Environmental Agency: 2014.
- (11) McLinden, M. O.; Brown, J. S.; Brignoli, R.; Kazakov, A. F.; Domanski, P. A. Limited Options for Low-Global-Warming-Potential Refrigerants. *Nat. Commun.* **2017**, *8*, 14476.
- (12) Castro, P. J.; Araújo, J. M.; Martinho, G.; Pereira, A. B. Waste Management Strategies to Mitigate the Effects of Fluorinated Greenhouse Gases on Climate Change. *Appl. Sci.* **2021**, *11* (10), 4367.
- (13) Lei, Z.; Dai, C.; Chen, B. Gas Solubility in Ionic Liquids. *Chem. Rev.* **2014**, *114* (2), 1289–1326.
- (14) Mellein, B. R.; Scurto, A. M.; Shiflett, M. B. Gas Solubility in Ionic Liquids. *Curr. Opin. Green Sust.* **2021**, *28*, 100425.
- (15) Shiflett, M. B.; Maginn, E. J. The Solubility of Gases in Ionic Liquids. *AIChE J.* **2017**, *63* (11), 4722–4737.
- (16) Blanchard, L. A.; Hancu, D.; Beckman, E. J.; Brennecke, J. F. Green Processing Using Ionic Liquids and CO₂. *Nature* **1999**, *399*, 28–29.
- (17) Cadena, C.; Anthony, J. L.; Shah, J. K.; Morrow, T. I.; Brennecke, J. F.; Maginn, E. J. Why is CO₂ so Soluble in Imidazolium-Based Ionic Liquids? *J. Am. Chem. Soc.* **2004**, *126* (16), 5300–5308.
- (18) Muldoon, M. J.; Aki, S. N.; Anderson, J. L.; Dixon, J. K.; Brennecke, J. F. Improving Carbon Dioxide Solubility in Ionic Liquids. *J. Phys. Chem. B* **2007**, *111* (30), 9001–9009.
- (19) Brennecke, J. F.; Maginn, E. Ionic liquids: Innovative Fluids for Chemical Processing. *AIChE J.* **2001**, *47* (11), 2384–2389.
- (20) Pereira, A. B.; Araújo, J. M. M.; Martinho, S.; Alves, F.; Nunes, S.; Matias, A.; Duarte, C. M. M.; Rebelo, L. P. N.; Marrucho, I. M. Fluorinated Ionic Liquids: Properties and Applications. *ACS Sustainable Chem. Eng.* **2013**, *1* (4), 427–439.
- (21) Pereira, A. B.; Araújo, J. M. M.; Esperança, J. M. S. S.; Rebelo, L. P. N. Surfactant Fluorinated Ionic Liquids. In *Ionic Liquid Devices – Smart Materials Series*; Eftekhari, A., Ed.; Royal Society of Chemistry, 2018; Vol. 4, pp 79–102. DOI: 10.1039/9781788011839-00079.
- (22) Vieira, N. S. M.; Ferreira, M. L.; Castro, P. J.; Araújo, J. M. M.; Pereira, A. B. Fluorinated Ionic Liquids as Task-Specific Materials: An Overview of Current Research. In *Ionic Liquids - Thermophysical Properties and Applications*; Mursheed, S. M. S., Ed.; IntechOpen, 2021. DOI: 10.5772/intechopen.96336.
- (23) Pereira, A. B.; Pastoriza-Gallego, M. J.; Shimizu, K.; Marrucho, I. M.; Canongia Lopes, J. N.; Piñeiro, M. M.; Rebelo, L. P. N. On the Formation of a Third, Nanostructured Domain in Ionic Liquids. *J. Phys. Chem. B* **2013**, *117* (37), 10826–10833.
- (24) Ferreira, M. L.; Pastoriza-Gallego, M. J.; Araújo, J. M. M.; Canongia Lopes, J. N.; Rebelo, L. P. N.; Piñeiro, M. M.; Shimizu, K.; Pereira, A. B. Influence of Nanosegregation on the Phase Behavior of Fluorinated Ionic Liquids. *J. Phys. Chem. C* **2017**, *121* (9), 5415–5427.
- (25) Vieira, N. S. M.; Reis, P. M.; Shimizu, K.; Cortes, O. A.; Marrucho, I. M.; Araújo, J. M. M.; Esperança, J. M. S. S.; Canongia Lopes, J. N.; Pereira, A. B.; Rebelo, L. P. N. A Thermophysical and Structural Characterization of Ionic Liquids with Alkyl and Perfluoroalkyl Side Chains. *RSC Adv.* **2015**, *5* (80), 65337–65350.
- (26) Luís, A.; Shimizu, K.; Araújo, J. M. M.; Carvalho, P. J.; Lopes-da-Silva, J. A.; Canongia Lopes, J. N.; Rebelo, L. P. N.; Coutinho, J. A. P.; Freire, M. G.; Pereira, A. B. Influence of Nanosegregation on the Surface Tension of Fluorinated Ionic Liquids. *Langmuir* **2016**, *32* (24), 6130–6139.
- (27) Vieira, N. S. M.; Luís, A.; Reis, P. M.; Carvalho, P. J.; Lopes-da-Silva, J. A.; Esperança, J. M. S. S.; Araújo, J. M. M.; Rebelo, L. P. N.; Freire, M. G.; Pereira, A. B. Fluorination Effects on the Thermodynamic, Thermophysical and Surface Properties of Ionic Liquids. *J. Chem. Thermodyn.* **2016**, *97*, 354–361.
- (28) Pereira, A. B.; Llovel, F.; Araújo, J. M. M.; Santos, A. S.; Rebelo, L. P. N.; Piñeiro, M. M.; Vega, L. F. Thermophysical Characterization of Ionic Liquids Based on the Perfluorobutanesulfonate Anion: Experimental and Soft-SAFT Modeling Results. *ChemPhysChem* **2017**, *18* (15), 2012–2023.
- (29) Ferreira, M. L.; Araújo, J. M. M.; Pereira, A. B.; Vega, L. F. Insights into the Influence of the Molecular Structures of Fluorinated Ionic Liquids on their Thermophysical Properties. A soft-SAFT based approach. *Phys. Chem. Chem. Phys.* **2019**, *21* (12), 6362–6380.
- (30) Bastos, J. C.; Carvalho, S. F.; Welton, T.; Lopes, J. N. C.; Rebelo, L. P. N.; Shimizu, K.; Araújo, J. M. M.; Pereira, A. B. Design of Task-Specific Fluorinated Ionic Liquids: Nanosegregation versus Hydrogen-Bonding Ability in Aqueous Solutions. *Chem. Commun.* **2018**, *54* (28), 3524–3527.
- (31) Teixeira, F. S.; Vieira, N. S. M.; Cortes, O. A.; Araújo, J. M. M.; Marrucho, I. M.; Rebelo, L. P. N.; Pereira, A. B. Phase Equilibria and Surfactant Behavior of Fluorinated Ionic Liquids with Water. *J. Chem. Thermodyn.* **2015**, *82*, 99–107.
- (32) Pereira, A. B.; Araújo, J. M. M.; Teixeira, F. S.; Marrucho, I. M.; Piñeiro, M. M.; Rebelo, L. P. N. Aggregation Behavior and Total Miscibility of Fluorinated Ionic Liquids in Water. *Langmuir* **2015**, *31* (4), 1283–1295.
- (33) Vieira, N. S. M.; Bastos, J. C.; Hermida-Merino, C.; Pastoriza-Gallego, M. J.; Rebelo, L. P. N.; Piñeiro, M. M.; Araújo, J. M. M.; Pereira, A. B. Aggregation and Phase Equilibria of Fluorinated Ionic Liquids. *J. Mol. Liq.* **2019**, *285*, 386–396.
- (34) Ferreira, M. L.; Araújo, J. M. M.; Vega, L. F.; Llovel, F.; Pereira, A. B. Functionalization of Fluorinated Ionic Liquids: A Combined Experimental-Theoretical Study. *J. Mol. Liq.* **2020**, *302*, 112489.
- (35) Pereira, A. B.; Araújo, J. M. M.; Martinho, S.; Alves, F.; Nunes, S.; Matias, A.; Duarte, C. M. M.; Rebelo, L. P. N.; Marrucho, I. M. Fluorinated Ionic Liquids: Properties and Applications. *ACS Sustainable Chem. Eng.* **2013**, *1* (4), 427–439.
- (36) Vieira, N. S. M.; Bastos, J. C.; Rebelo, L. P. N.; Matias, A.; Araújo, J. M. M.; Pereira, A. B. Human Cytotoxicity and Octanol/Water Partition Coefficients of Fluorinated Ionic Liquids. *Chemosphere* **2019**, *216*, 576–586.
- (37) Ferreira, M. L.; Vieira, N. S. M.; Araújo, J. M. M.; Pereira, A. B. Unveiling the Influence of Non-Toxic Fluorinated Ionic Liquids Aqueous Solutions in the Encapsulation and Stability of Lysozyme. *Sustain. Chem.* **2021**, *2* (1), 149–166.
- (38) Vieira, N. S. M.; Stolte, S.; Araújo, J. M. M.; Rebelo, L. P. N.; Pereira, A. B.; Markiewicz, M. Acute Aquatic Toxicity and Biodegradability of Fluorinated Ionic Liquids. *ACS Sustainable Chem. Eng.* **2019**, *7* (4), 3733–3741.
- (39) Vieira, N. S. M.; Oliveira, A. L.; Araújo, J. M. M.; Gaspar, M. M.; Pereira, A. B. Ecotoxicity and Hemolytic Activity of Fluorinated Ionic Liquids. *Sustain. Chem.* **2021**, *2* (1), 115–126.
- (40) Sosa, J. E.; Ribeiro, R. P. P. L.; Castro, P. J.; Mota, J. P. B.; Araújo, J. M. M.; Pereira, A. B. Absorption of Fluorinated Greenhouse Gases Using Fluorinated Ionic Liquids. *Ind. Eng. Chem. Res.* **2019**, *58* (45), 20769–20778.
- (41) Lepre, L. F.; Pison, L.; Otero, I.; Gautier, A.; Dévemy, J.; Husson, P.; Pádua, A. A. H.; Gomes, M. C. Using Hydrogenated and Perfluorinated Gases to Probe the Interactions and Structure of

- Fluorinated Ionic Liquids. *Phys. Chem. Chem. Phys.* **2019**, *21* (17), 8865–8873.
- (42) Lepre, L. F.; Andre, D.; Denis-Quanquin, S.; Gautier, A.; Pádua, A. A. H.; Gomes, M. C. Ionic Liquids Can Enable the Recycling of Fluorinated Greenhouse Gases. *ACS Sustainable Chem. Eng.* **2019**, *7* (19), 16900–16906.
- (43) Castro, P. J.; Redondo, A. E.; Sosa, J. E.; Zakrzewska, M. E.; Nunes, A. V. M.; Araújo, J. M. M.; Pereiro, A. B. Absorption of Fluorinated Greenhouse Gases in Deep Eutectic Solvents. *Ind. Eng. Chem. Res.* **2020**, *59* (29), 13246–13259.
- (44) Jovell, D.; Gómez, S. B.; Zakrzewska, M. E.; Nunes, A. V. M.; Araújo, J. M. M.; Pereiro, A. B.; Llovel, F. Insight on the Solubility of R134a in Fluorinated Ionic Liquids and Deep Eutectic Solvents. *J. Chem. Eng. Data* **2020**, *65* (10), 4956–4969.
- (45) Vega, L. F.; Vilaseca, O.; Llovel, F.; Andreu, J. S. Modeling Ionic Liquids and the Solubility of Gases in them: Recent Advances and Perspectives. *Fluid Phase Equilib.* **2010**, *294* (1–2), 15–30.
- (46) Alkhatib, I. I. I.; Bahamon, D.; Llovel, F.; Abu-Zahra, M. R.; Vega, L. F. Perspectives and Guidelines on Thermodynamic Modelling of Deep Eutectic Solvents. *J. Mol. Liq.* **2020**, *298*, 112183.
- (47) Sosa, J. E.; Santiago, R.; Hospital-Benito, D.; Gomes, M. C.; Araújo, J. M. M.; Pereiro, A. B.; Palomar, J. Process Evaluation of Fluorinated Ionic Liquids as F-Gas Absorbents. *Environ. Sci. Technol.* **2020**, *54* (19), 12784–12794.
- (48) Blas, F. J.; Vega, L. F. Thermodynamic Behaviour of Homonuclear and Heteronuclear Lennard-Jones Chains with Association Sites from Simulation and Theory. *Mol. Phys.* **1997**, *92* (1), 135–150.
- (49) Blas, F. J.; Vega, L. F. Prediction of Binary and Ternary Diagrams Using the Statistical Associating Fluid Theory (SAFT) Equation of State. *Ind. Eng. Chem. Res.* **1998**, *37* (2), 660–674.
- (50) Ferreira, M. L.; Llovel, F.; Vega, L. F.; Pereiro, A. B.; Araújo, J. M. M. Systematic Study of the Influence of the Molecular Structure of Fluorinated Ionic Liquids on the Solubilization of Atmospheric Gases Using a Soft-SAFT Based Approach. *J. Mol. Liq.* **2019**, *294*, 111645.
- (51) Asensio-Delgado, S.; Jovell, D.; Zarca, G.; Urriaga, A.; Llovel, F. Thermodynamic and Process Modeling of the Recovery of R410A Compounds with Ionic Liquids. *Int. J. Refrig.* **2020**, *118*, 365–375.
- (52) Andreu, J. S.; Vega, L. F. Capturing the Solubility Behavior of CO₂ in Ionic Liquids by a Simple Model. *J. Phys. Chem. C* **2007**, *111* (43), 16028–16034.
- (53) Llovel, F.; Valente, E.; Vilaseca, O.; Vega, L. F. Modeling Complex Associating Mixtures with [C_n-mim][Tf₂N] Ionic Liquids: Predictions from the Soft-SAFT Equation. *J. Phys. Chem. B* **2011**, *115* (15), 4387–4398.
- (54) Pereira, L. M. C.; Oliveira, M. B.; Dias, A. M. A.; Llovel, F.; Vega, L. F.; Carvalho, P. J.; Coutinho, J. A. P. High Pressure Separation of Greenhouse Gases from Air with 1-Ethyl-3-Methylimidazolium Methyl-Phosphonate. *Int. J. Greenhouse Gas Control* **2013**, *19*, 299–309.
- (55) Llovel, F.; Oliveira, M. B.; Coutinho, J. A. P.; Vega, L. F. Solubility of Greenhouse and Acid Gases on the [C₄mim][MeSO₄] Ionic Liquid for Gas Separation and CO₂ conversion. *Catal. Today* **2015**, *255*, 87–96.
- (56) Alonso, G.; Gamallo, P.; Sayós, R.; Llovel, F. Combining Soft-SAFT and COSMO-RS Modeling Tools to Assess the CO₂–SO₂ Separation Using Phosphonium-Based Ionic Liquids. *J. Mol. Liq.* **2020**, *297*, 111795.
- (57) Albà, C. G.; Vega, L. F.; Llovel, F. Assessment on Separating Hydrofluoroolefins from Hydrofluorocarbons at the Azeotropic Mixture R513A by Using Fluorinated Ionic Liquids: A Soft-SAFT Study. *Ind. Eng. Chem. Res.* **2020**, *59* (29), 13315–13324.
- (58) Ojeda, R. M.; Llovel, F. Soft-SAFT Transferable Molecular Models for the Description of Gas Solubility in Eutectic Ammonium Salt-Based Solvents. *J. Chem. Eng. Data* **2018**, *63* (7), 2599–2612.
- (59) Lloret, J. O.; Vega, L. F.; Llovel, F. Accurate Description of Thermophysical Properties of Tetraalkylammonium Chloride Deep Eutectic Solvents with the Soft-SAFT Equation of State. *Fluid Phase Equilib.* **2017**, *448*, 81–93.
- (60) Vilaseca, O.; Llovel, F.; Yustos, J.; Marcos, R. M.; Vega, L. F. Phase Equilibria, Surface Tensions and Heat Capacities of Hydrofluorocarbons and their Mixtures Including the Critical Region. *J. Supercrit. Fluids* **2010**, *55* (2), 755–768.
- (61) Dias, A. M.; Pámies, J. C.; Coutinho, J. A.; Marrucho, I. M.; Vega, L. F. SAFT Modeling of the Solubility of Gases in Perfluoroalkanes. *J. Phys. Chem. B* **2004**, *108* (4), 1450–1457.
- (62) Albà, C. G.; Vega, L. F.; Llovel, F. A Consistent Thermodynamic Molecular Model of n-Hydrofluoroolefins and Blends for Refrigeration Applications. *Int. J. Refrig.* **2020**, *113*, 145–155.
- (63) Chapman, W. G.; Gubbins, K. E.; Jackson, G.; Radosz, M. SAFT: Equation-of-state Solution Model for Associating Fluids. *Fluid Phase Equilib.* **1989**, *52*, 31–38.
- (64) Chapman, W. G.; Gubbins, K. E.; Jackson, G.; Radosz, M. New Reference Equation of State for Associating Liquids. *Ind. Eng. Chem. Res.* **1990**, *29* (8), 1709–1721.
- (65) Huang, S. H.; Radosz, M. Equation of State for Small, Large, Polydisperse, and Associating Molecules. *Ind. Eng. Chem. Res.* **1990**, *29* (11), 2284–2294.
- (66) Johnson, J. K.; Zollweg, J. A.; Gubbins, K. E. The Lennard-Jones Equation of State Revisited. *Mol. Phys.* **1993**, *78* (3), 591–618.
- (67) Wertheim, M. S. Fluids with Highly Directional Attractive Forces. I. Statistical Thermodynamics. *J. Stat. Phys.* **1984**, *35*, 19–34.
- (68) Wertheim, M. S. Fluids with Highly Directional Attractive Forces. II. Thermodynamic Perturbation Theory and Integral Equations. *J. Stat. Phys.* **1984**, *35*, 35–47.
- (69) Wertheim, M. S. Fluids with Highly Directional Attractive Forces. III. Multiple Attraction Sites. *J. Stat. Phys.* **1986**, *42*, 459–476.
- (70) Wertheim, M. S. Fluids with Highly Directional Attractive Forces. IV. Equilibrium Polymerization. *J. Stat. Phys.* **1986**, *42*, 477–492.
- (71) Alkhatib, I. I. I.; Pereira, L. M. C.; Torne, J.; Vega, L. F. Polar soft-SAFT: Theory and Comparison with Molecular Simulations and Experimental Data of Pure Polar Fluids. *Phys. Chem. Chem. Phys.* **2020**, *22* (23), 13171–13191.
- (72) Alkhatib, I. I. I.; Vega, L. F. Quantifying the Effect of Polarity on the Behavior of Mixtures of n-Alkanes with Dipolar Solvents using Polar soft-SAFT. *AIChE J.* **2021**, *67* (3), e16649.
- (73) Vega, L. F.; Bahamon, D.; Alkhatib, I. I. I.; Fouad, W. A.; Llovel, F.; Pereira, L. M. C.; Vilaseca, O. How Molecular Modelling Tools Can Help in Mitigating Climate Change. In *Foundations of Molecular Modeling and Simulation. Molecular Modeling and Simulation (Applications and Perspectives)*; Maginn, E. J.; Errington, J., Eds.; Springer: Singapore, 2021. DOI: 10.1007/978-981-33-6639-8_8.
- (74) Cadena, C.; Anthony, J. L.; Shah, J. K.; Morrow, T. I.; Brennecke, J. F.; Maginn, E. J. Why is CO₂ so soluble in imidazolium-based ionic liquids? *J. Am. Chem. Soc.* **2004**, *126* (16), 5300–5308.
- (75) Marciniak, A. The Hildebrand solubility parameters of ionic liquids—part 2. *Int. J. Mol. Sci.* **2011**, *12* (6), 3553–3575.